

Pressure-temperature phase diagrams of stage-2–4 potassium-graphite intercalation compounds deduced from anomalies in the basal-plane resistivity

B. Sundqvist

Department of Physics, University of Umeå, S-901 87 Umeå, Sweden

J. E. Fischer

Materials Science and Engineering Department and Laboratory for Research on the Structure of Matter, University of Pennsylvania, Philadelphia, Pennsylvania 19104

(Received 11 December 1986)

The basal-plane resistivities ρ of stage-2–4 potassium-graphite intercalation compounds (K-GIC's) have been measured as functions of temperature T and pressure p using a contactless method. The pressure range investigated was 0–1.4 GPa. For stage-2 K-GIC (KC₂₄) measurements were made in the temperature range 90–300 K, while for the higher-stage materials the range was mainly limited to 245–300 K. In all cases ρ increases with p through the anomalous regime near the phase transitions, whereas $d\rho/dp$ is always negative in the stable high- p (high-stage) phases. Approximate p - T phase diagrams are deduced from anomalies in ρ corresponding to the staging and in-plane order-disorder transitions, respectively. In all cases the slopes dp/dT of the phase boundaries for the high-pressure staging transitions are such that the transitions extrapolate to positive T at atmospheric p , although no such transitions have been reported. The low- p staging-ordering phase boundary of KC₂₄ is particularly complex, involving segments with both $dp/dT \rightarrow 0$ ($125 < T < 200$ K) and $dp/dT \rightarrow \infty$ ($T \approx 125$ K). The p - T diagrams are compared with recent structural experiments and models. We suggest that the complexity of the KC₂₄ phase diagram is attributable to the weakly incommensurate in-plane structure at low p and T .

I. INTRODUCTION

Although potassium-graphite is one of the best investigated of all graphite intercalation compound (GIC) systems, there are still large gaps in our knowledge. Alkali-metal GIC's exhibit^{1,2} a variety of structural phase transitions as functions of metal density, temperature T , and pressure p , and many such transitions can be understood from simple thermodynamic models. As an example, LiC₁₆ transforms from stage 2 at 300 K, 0.1 MPa (atmospheric pressure) to a mixture of stage 2 and stage 3 at either 245 K, 0.1 MPa or 300 K, 0.3 GPa (3 kbar). (Stage n indicates that there are n graphite monolayers between each intercalate layer.) The staging transition is accompanied by a change in areal density from an open structure with roughly 25% vacant sites in each intercalate layer to an ordered commensurate close-packed $\sqrt{3} \times \sqrt{3}$ superlattice. DiVincenzo *et al.*³ calculated the slope dp/dT of the corresponding phase boundary in the p - T phase diagram from the thermodynamic relation $dp/dT = dS/dV$, using a mean-field approximation for the configurational entropy. The result, $dp/dT = 5.6$ MPa/K, is identical to the slope found experimentally, implying that the relevant energies are independent of T and p . Even simpler phase diagrams are found⁴ in the acceptor system HNO₃-graphite, where all sites are occupied, making staging and in-plane densification impossible: Low-stage ($2 \leq n \leq 4$) HNO₃ GIC's exhibit an in-plane ordering transition at $T_c \approx 250$ K, 0.1 MPa, the same transition also occurring at 300 K and 0.4 GPa.

The potassium-graphite system is more complicated,

and several phase transitions are known to occur as functions of T or p . For stages-2–4 K-GIC's combined staging and in-plane ordering transitions are found^{5–7} at high pressures near 300 K, in agreement with simple theory.^{3,8} At atmospheric pressure, on the other hand, two different transitions are known to occur in all three materials at $T < 300$ K, but these transitions involve^{9–12} only potassium in-plane ordering and changes in the stacking sequence, and no low- T staging transitions have been observed. The high- T –high- p behavior of K GIC's thus differs significantly from that at low T and low p , and there has been no reason to suspect that the high- p staging transitions in these materials should be connected with the low- T ordering transitions.

Neutron scattering experiments⁷ on K-GIC's show that restaging at high p occurs through a combination of continuous and abrupt processes, starting at pressures below 0.1 GPa. As an example, for KC₂₄ there is an abrupt increase⁷ in the proportion of stage 3 (to well over 50%) at 0.35 GPa. Using the model of DiVincenzo *et al.*,³ with the entropy calculated from a dilute lattice-gas model at low p , we estimate a slope $dp/dT \approx 1$ MPa/K for the corresponding phase boundary. This slope is much smaller than for LiC₁₆, due to the larger volume per K site, and implies that this transition extrapolates to ≈ 0 K at $p = 0$. However, in the case of K-GIC's the true dS is probably larger than that given by the lattice-gas model so the transition should, in fact, occur at some $T > 0$ at $p = 0$. Regardless of the reliability of the estimated dp/dT , the absence of a low- T staging transition is also quite puzzling because the pressure-induced staging transition starts⁷

below 0.1 GPa at 300 K.

We were thus stimulated to investigate the p - T phase diagrams of stages-2–4 K-GIC's, and we report here the results of this investigation, which was carried out through measurements of the basal-plane resistivity ρ as a function of T and p in the range 90–300 K and 0–1.4 GPa. The phase diagrams were mapped through the anomalies observed in ρ at the various transitions involved. As described in a preliminary report¹³ we have found that the 0.35-GPa resistance anomaly (and staging transition) in KC_{24} is actually connected by a continuous boundary to the in-plane ordering transition at $T_u = 125$ K. Near 300 K this boundary is linear and extrapolates exactly to T_u , but at lower T it curves away from the T axis such that $dp/dT \rightarrow 0$ below 150 K, and is then connected by a short segment with very large dp/dT to T_u at 0 GPa. We have also mapped the phase boundaries for the 0.75-GPa anomaly^{6,7} and for the low- T anomaly at T_l .⁹ For comparison, the high-temperature part ($T > 245$ K) of the phase diagrams for KC_{36} and KC_{48} has also been studied. In all cases we find that the staging transitions extrapolate to $T > 0$ K at 0.1 MPa, in direct contradiction to the experimental evidence at low p and low T .

The paper is organized as follows. In Sec. II we briefly describe our experimental method and equipment. Section III is devoted to a description of, and a discussion of, our experimental results for (initially) stage-2 K-GIC, while Sec. IV deals with stages 3 and 4 K-GIC's in a similar way. This is followed by Sec. V, containing some general conclusions.

II. EXPERIMENTAL DETAILS

The samples studied were approximately $5 \times 5 \times 0.5$ mm³ and were based on highly oriented pyrolytic graphite (HOPG). They were intercalated at the University of Pennsylvania in Philadelphia using the standard two-zone vapor method¹ and characterized by x-ray diffraction before being shipped to Umeå in sealed glass tubes for the high- p measurements. The glass tubes were always opened under Ar gas in a glove bag, where the sample thickness d was measured before the sample was transferred to the liquid-filled pressure cell, a procedure that usually took less than a minute. After each run the samples were returned to the same glass capsules.

The basal-plane resistivity ρ was measured using a recently developed contactless method described elsewhere.^{14,15} Although the absolute accuracy obtained is not very good, relative changes can be measured with high precision. The resolution was usually better than 0.1% near 300 K and better than 0.03% near 100 K. Since the quantity measured is actually d/ρ we must correct the measured data for the c -axis compression in order to find the true pressure dependence of ρ .

After each experiment ρ always returned to within 2% of the original value at 0.1 MPa. It was obvious from the color of the KC_{24} samples, however, that some stage-3 phase was present after the runs. Some samples were therefore returned to Philadelphia for x-ray analysis, which in all cases showed less than 10% admixture of stage 3. (The corresponding deintercalation was probably

caused by reaction with water or oxygen dissolved in the pressure medium.) The presence of 10% of the stage-3 phase in an otherwise stage-2 sample might possibly modify the phase diagram through the resulting stage disorder. This was checked by studying one KC_{24} sample in three different experiments, first as a virgin sample, and later twice after a return trip to Philadelphia for x-ray analysis. In all three experiments the absolute value of ρ , its p and T dependence, as well as the location of the phase boundaries, were identical to within the experimental errors over the range $100 \text{ K} < T < 300 \text{ K}$ and at all p . Small amounts of stage disorder thus do not affect the phase diagram of KC_{24} as reflected in the measured ρ .

The high-pressure equipment has also been described elsewhere.¹⁵ In most experiments the pressure medium used was a 50-50 mixture of n -pentane and isopentane, since this medium has excellent hydrostatic properties to below 150 K. Near 300 K pure n -pentane or silicone oil (1 mm²/s Dow Corning DC200 fluid) was sometimes used. No significant change in ρ due to contamination was observed before or during any pressure run. T was measured with a type-K thermocouple to within 0.2 K at 300 and 1 K at lower T (due to temperature gradients), while p was measured by an *in situ* Manganin gauge calibrated to within 1% at 300 K. (Below 200 K the accuracy is assumed to be 2%.) The pressure medium always solidified at 120–140 K, depending on p . This could easily be observed from the Manganin resistance which is very sensitive to anisotropic strain. Below the glass transition of the medium p was calculated from an empirical pressure-versus-load curve believed to be accurate to within 0.015 GPa or 5%, whichever is larger. In this range accurate data for ρ could only be obtained from isobaric measurements of $\rho(T)$, since the strain induced in the coil system when changing p caused very large changes in output phase and voltage. A few attempts were made to measure $\rho(p)$ near 110 K, as discussed in Sec. III, but the results were, at best, ambiguous.

III. EXPERIMENTAL RESULTS AND DISCUSSION: STAGE-2 K-GIC

A. Structure and phases of stage-2 K-GIC

At 300 K and 0.1 MPa stage-2 K-GIC has the nominal composition KC_{24} , but pure stage 2 is found for compositions ranging⁷ from KC_{23} to KC_{28} . [However, here and in the following we shall often use the shorter expression KC_x , with $x = 24, 36$, and 48, to denote stage-(2–4) K-GIC's, without implying that the materials have these exact compositions.] The in-plane structure may be described^{1,16} as liquidlike, with no long-range order but some degree of short-range order and some orientational correlation with the graphite network. At 0.1 MPa there are two phase transitions at low T , correlated with anomalies^{9,17} in both ρ and the c -axis resistivity ρ_c . These were first attributed by Hastings *et al.*¹⁰ to in-plane ordering at $T_u \approx 125$ K and a change in stacking at $T_l \approx 95$ K. Below T_u the K atoms are believed¹⁸ to form regular commensurate $\sqrt{7} \times \sqrt{7}$ (or¹² $\sqrt{201} \times \sqrt{201}$) superlattices within hexagonal domains separated by discommensura-

tions. (In this model the high- T structure results from a gradual randomization of the discommensuration domains with increasing T .) Below T_1 , however, recent work by Rousseaux *et al.*,¹¹ Winokur and Clarke,¹² and Cajipe and Fischer¹⁹ show that the situation is more complicated. Apart from a change in the c -axis stacking sequence¹⁰ there is an intralayer K reordering¹¹ to a complex, probably commensurate ordered phase.¹² Small variations in the K-C ratio, however, can produce large differences in structure.¹⁹

At 300 K KC_{24} transforms at high p into an ordered stage-3 phase with a commensurate 2×2 K superlattice.^{2,5} The transformation occurs through a mixture of continuous and abrupt processes.^{6,7} The proportion of stage 3 increases⁷ with p from zero at 0.1 MPa to approximately 40% at 0.34 GPa, where there is an abrupt increase to 65% at constant p . A corresponding anomaly in ρ_c is reported⁶ at 0.35 ± 0.02 GPa. The amount of stage-3 material then continues to increase slowly until at 0.7 GPa there is a final, abrupt transformation to almost pure stage 3, again correlated with a large anomaly in ρ_c at 0.75 ± 0.04 GPa.

B. Pressure and temperature dependence of the basal plane resistivity of KC_{24}

In all, five samples were studied, but only four of these under pressure. The measured ρ at STP was $8 \pm 2 \mu\Omega \text{cm}$, in good agreement with literature^{9,20} values, except for one sample which had $\rho = 13.6 \mu\Omega \text{cm}$. This high apparent ρ was probably due to some mechanical flaw in the sample, since the measured $\rho(p)$ unambiguously indicated a stage-2 sample.

Figure 1 shows ρ versus p for one sample at 293 K. (All results shown in the figures are uncorrected for c -axis compression.) Two anomalies are immediately obvious, one consisting of a drop in ρ at 0.32 GPa, the second a large increase in ρ with p terminating in a plateau above 0.7 GPa. These anomalies are readily identified as the abrupt parts of the staging transition discussed in the

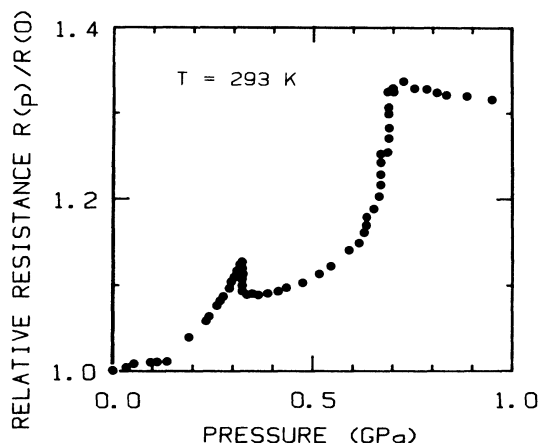


FIG. 1. Relative resistance $R(p)/R(0)$ vs p for one KC_{24} sample.

preceding section. The general features of $\rho(p)$ can be explained from the results of Kim *et al.*⁷ Near $p=0$, ρ depends little on p , as would be expected for a metallic material like KC_{24} . Already below 0.15 GPa, however, the staging transition starts,⁷ and part of the increase in ρ between 0.15 and 0.32 GPa is doubtless caused by increasing stage disorder. The sharp drop at 0.32 GPa corresponds to a sudden increase⁷ in the amount of stage-3 material. A similar drop in ρ_c occurs at the same pressure.⁶ Between 0.32 and 0.6 GPa the amount of stage 3 increases, which is reflected in a corresponding increase in ρ , until at about 0.7 GPa the sample is transformed into virtually pure⁷ stage 3. In the stage-3 phase, ρ decreases linearly with increasing p up to at least 1.4 GPa (not shown on plot). Extrapolating back to $p=0$ we find ρ to be 30% to 50% larger for stage-3 KC_{24} than for stage 2. The sharp rise in ρ immediately below 0.7 GPa can be described as a percolation phenomenon:²¹ Since the resistivity of the stage-2 phase is substantially lower than that of the stage-3 phase, the effective ρ will depend mainly on the resistivity of the stage-2 phase as long as there is a continuous stage-2 matrix in the sample. Not until quite near the end of the transition will most of the stage-2 channels break up, causing the effective ρ to rise toward the stage-3 value. The two anomalies will be discussed further in the following subsections. We only note here that ρ decreases at 0.32 GPa, in spite of the fact that a large proportion of the stage-2 material simultaneously transforms into stage-3 material with more than a 30% higher resistivity.

For the pure stage-3 phase above 0.7 GPa $d\rho/dp$ was always negative. For the results shown in Fig. 1, $d\rho/dp = -0.052 \mu\Omega \text{cm/GPa}$, and the pressure coefficient of ρ , defined as

$$\gamma = [1/\rho(0)]d\rho/dp, \quad (1)$$

was $\gamma = -0.050 \text{ GPa}^{-1}$. In most experiments $d\rho/dp$ for this phase was measured only over a small range in p , but between 110 and 300 K, $d\rho/dp$ was always negative and $|\gamma|$ mostly larger than 0.05 (see Fig. 3 below). Since $\rho(p)$ was usually slightly nonlinear immediately above the transition, we take $\gamma = -0.050 \text{ GPa}^{-1}$ as our best estimate of the true γ near 300 K. The c -axis compressibility k_c of the stage-3 phase is⁷ approximately 0.037 GPa^{-1} , from which we obtain a corrected ("true") value of $\gamma = -0.09 \text{ GPa}^{-1}$. This value is similar to that for⁴ stages ≥ 4 HNO_3 GIC's but differs even in sign from data for most low-stage acceptor compounds.^{4,15,22}

The resistivity of GIC's is usually assumed to be dominated by electron-phonon scattering,²³ like in most other metallic materials, but due to various imperfections in the material there is also usually a large residual resistivity. It has recently been suggested²⁴ that the latter is dominated by electron scattering from Daumas-Hérold domain²⁵ walls, and that the pressure dependence of this mechanism should add significantly to the observed pressure dependence of ρ . However, since the residual resistivity in our case is less than 10% of ρ near 300 K, even a strong pressure dependence of this term would have little effect on the total measured γ , and in our analysis we shall assume ρ to be dominated by electron-phonon scattering. (In principle, our measurements at low T might show effects

of domain size changes,²⁴ but in practice our data are not accurate enough.) $\rho(p)$ will then depend on the combined effects of pressure on the phonon spectrum and on the electron band structure, respectively. The influence of the change in the phonon spectrum can be estimated from the well-known expression²⁶

$$d(\ln\rho)/d(\ln V) = 2\gamma_G, \quad (2)$$

where γ_G is the Grüneisen parameter. Little is known about γ_G for GIC's, but for pure graphite it is extremely anisotropic²⁷ ($\gamma_G = -1.0$ in the plane and $+0.5$ along the c axis) with a bulk or mean value of 0.25. For GIC's the in-plane value should be similar to that of pure graphite, and for KC_{24} the c -axis value is²⁸ 0.86. The bulk γ_G is thus probably about 0.5, making the theoretical $d(\ln\rho)/d(\ln V) \approx 1$, significantly smaller than the experimental result 2.35. Still ignoring any pressure effects on the small residual resistivity (see above) we conclude that the effect of pressure on the electron band structure is more important than its effect on the phonon spectrum in determining $\rho(p)$ in stage-3 KC_{24} . (This is also the case for pure graphite²⁹ and most acceptor GIC's.^{4,22}) The lack of data on band structures for the high- p phases of K-GIC's makes a further discussion impossible at present. [Note, also, that the reverse conclusion is not possible: If the experimental value for $d(\ln\rho)/d(\ln V)$ equals that calculated from Eq. (2), this might be a coincidence, and $\rho(p)$ might still be determined mainly by band structure changes with pressure.]

For the low- p stage-2 phase we cannot measure $d\rho/dp$. The staging transition is reported⁷ to start below 0.1 GPa, and the results shown in Fig. 1 show a sharp break in $d\rho/dp$ at 0.15 GPa that might be connected with this feature. Similar results ($\rho = \text{const}$ to 0.1–0.15 GPa, followed by a step in $d\rho/dp$) were obtained for three samples. This might indicate that the staging transition sometimes starts at slightly higher pressures than those given by Kim *et al.*⁷ If this interpretation is correct $|d\rho/dp| \approx 0$ in the pure stage-2 phase, with the true γ small and negative.

In contrast to the nonlinear behavior of $\rho(p)$, ρ was almost linear in T , in agreement with literature data.^{9,23,30} A small T^2 term was evident only in measurements over large ranges in T . Figure 2 shows some typical isobaric results, chosen to show the typical behavior of $\rho(T)$ at the various transitions mentioned in Sec. IIIA. Curve A shows the same transition (arrow) as that at 0.7 GPa in Fig. 1. The two curves are radically different: The large step anomaly of Fig. 1 is reduced to a change in $d\rho/dT$ in Fig. 2. Curves B and F show the same transition as that observed in Fig. 1 at 0.32 GPa, and curve E shows the anomaly at T_l only. Curve G shows the anomalies at both T_u and T_l , as obtained at 80 MPa. The anomalies in these curves are quite similar to those found previously by Onn *et al.*⁹ at 0.1 MPa. Curves C and D, at 0.65 and 0.07 GPa, respectively, show the T dependence of ρ over large ranges in T in the (almost) pure stage-3 and stage-2 phases, respectively.

Both $d\rho/dT$ and the temperature coefficient of resistivity were different for different stages, and also varied between samples. Data for $\rho(T)$ were obtained for three

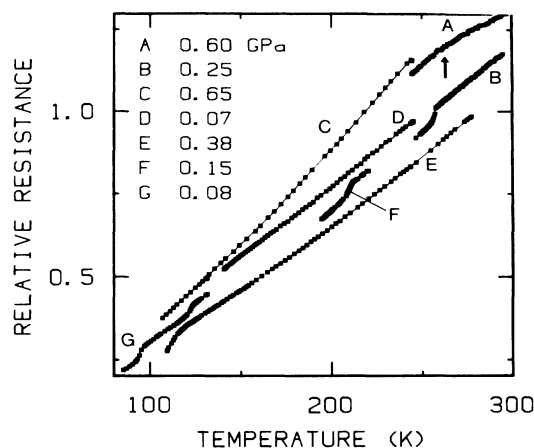


FIG. 2. Relative resistance $R(p, T)/R(0, 293)$ vs T for several KC_{24} samples at the pressures indicated. Curves C and D have been displaced upward and curve E downward to avoid overlap. The arrow indicates the staging transition at 0.60 GPa.

samples. For two of these $d\rho/dT$ was approximately $0.05 \mu\Omega \text{ cm/K}$ in stage 2 at low p , and $> 0.11 \mu\Omega \text{ cm/K}$ in the stage-3 phase, while for the third $d\rho/dT$ was slightly smaller ($0.04 \mu\Omega \text{ cm/K}$) at low p , and significantly smaller ($0.05 \mu\Omega \text{ cm/K}$) in the stage-3 phase. These figures are all valid near 300 K, but due to the quadratic term in T evident in curves C-E in Fig. 2 $d\rho/dT$ was up to 35% lower near 100 K. No systematic difference was detected between the values of $d\rho/dT$ above and below T_u . These data are all compatible with the results of Onn *et al.*⁹ Although ρ for the stage-3 phase was 30–50% higher than that of the stage-2 phase at 295 K, the higher $d\rho/dT$ of the former led to the two resistivities being approximately equal near 100 K. Between 0.1 and 0.5 GPa, $d\rho/dT$ was observed to increase with increasing p , both above and below the anomaly. This was attributed to the increasing proportion of the stage-3 phase.

It has been suggested²⁵ that KC_{24} may be a superconductor at very low T , but no indications of this have been found^{2,31} for $p < 1$ GPa and $T > 70$ mK. We note that for metals, the p dependence of the electron-phonon interaction parameter, and thus T_c , can be calculated³² from $\rho(p, T)$, provided band structure effects are taken into account. In principle our results for $\rho(p, T)$ in the high- p phase could be used to calculate whether dT_c/dp is positive or negative, i.e., whether there is any hope that KC_{24} might become superconducting under pressure. In practice we do not know enough about the band structure at high p to give a definite answer to that question. The negative $d\rho/dp$, however, might indicate³² that the electron-phonon interaction decreases with increasing p , and thus that no superconductivity should be expected under pressure.

C. Phase boundary for the 0.7 GPa anomaly (end of staging transition)

As demonstrated by Fig. 3 the upper anomaly in ρ could easily be traced as a function of T . The data shown

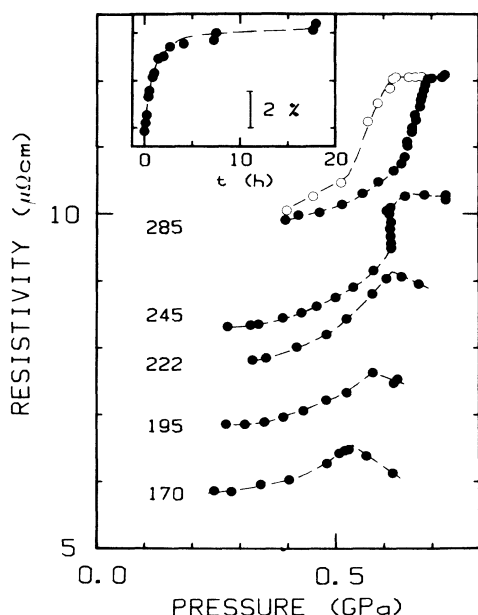


FIG. 3. Resistivity vs p for one single KC_{24} sample at the temperatures (in K) indicated. Filled symbols indicate increasing p , open symbols decreasing p . The inset shows the data for $\rho(t)$ at 245 K and 0.6 GPa plotted vs time t .

are for one single sample and mainly for increasing p , but one set of data (open symbols at 285 K) is shown for decreasing p to show the hysteresis. The transition pressure p_s was defined as the final sharp break in ρ , or, if this was not possible, as the intersection of two lines fitted above and below the anomaly. The final rise in ρ near p_s was rather sluggish. At $T > 200$ K we could almost always observe a slow, upward drift in ρ if p was kept constant within about 0.1 GPa below p_s , and a typical curve for $\rho(t)$ (at 245 K) is shown in the inset. The drift persists for several hours and ρ seems to saturate at a value below that for the stage-3 phase. The equilibrium phase at this T and p is therefore probably still a mixture of stages 2 and 3, and the “pure” stage-3 phase is not obtained until at some higher, well-defined pressure ($\approx p_s$). The t dependence made it difficult to obtain accurate values for p_s . Above p_s , however, all systematic t dependence disappeared, in agreement with the results of Kim and Fischer.³³ Also, well below p_s , ρ is dominated by the resistivity of the stage-2 phase and no t dependence is observed, since small changes in the composition of the sample does not affect the effective ρ . Similarly, below 200 K the resistivities of the phases are almost equal and no drift with t can be observed.

The change in ρ at p_s gets smaller at low T as would be expected from the difference in $d\rho/dT$ between phases. We could follow the transition down to below 150 K, but below this the pressure medium was no longer hydrostatic at p_s and changes in p caused strains which made accurate measurements impossible. Above 150 K we have

mapped the phase boundaries corresponding to the upper anomaly in ρ for both increasing and decreasing p . All measured values for p_s in this range were weighted according to the estimated error in the measurement and fitted to a linear function of T . For increasing p the mean transition pressure was 0.74 ± 0.02 GPa at 300 K with a phase boundary slope $dp/dT = 1.7$ MPa/K, while for decreasing p the corresponding values were 0.67 ± 0.02 GPa and 1.9 MPa/K. The hysteresis thus tends to increase slightly at lower T . For increasing p , all experimental points except one (Fig. 1) were within 30 MPa (4%) of these lines, with a slightly larger scatter for decreasing p . The transition pressures are in excellent agreement with literature data.^{6,7}

For stage-2 LiC_{16} the slope of the phase boundary corresponding to the staging transition can be calculated from a mean field theory for the entropies of the two phases.³ Applying the same calculation in the present case, and in particular assuming a dilute lattice gas model at low p and zero entropy in the high-pressure phase, the difference in site volume between K and Li atoms will result in a slope of approximately 1 MPa/K, or 60% of the observed value. The difference is not very surprising since the lattice gas model is not a very good description of the low- p state of the material. Recent calculations support a model¹⁸ in which some amount of short-range order persists even at room temperature. The configurational entropy of the low- p phase is thus probably in between the low value of the ordered lattice gas model and the high value of a completely disordered liquid, leading to a value for dp/dT in better agreement with experiment.

D. Phase boundary for the T_u ordering transition

The shape of the 0.32 GPa anomaly in Fig. 1 is typical⁴ of an order-disorder-type transformation. Cooling through the same transition at $T > 200$ K and $p > 0.2$ GPa produced curves of the more familiar type⁹ shown in Fig. 2 (B,F,G). The step change in ρ , $\Delta\rho$, was between 0.1 and $0.6 \mu\Omega \text{ cm}$, depending on the sample, but with no systematic dependence on either t , T , or p . The transitions were quite rapid. At the actual transition point ρ decreased toward the final value with a time constant of a couple of minutes, but increasing p further by a few MPa usually completed the transition within seconds. Below the anomaly ρ was perfectly stable with t over at least 24 h but above the anomaly a small, slow drift with t was sometimes observed. Fitting all transition points in the range 200 to 300 K to linear functions of T gave mean transition pressures at 300 K of 0.332 ± 0.005 GPa for increasing p and 0.300 ± 0.005 GPa for decreasing p . The agreement between different samples, and between different runs on the same sample, was excellent, with only two points differing by more than 10 MPa (3%) from the curves. The slopes dp/dT of the phase boundaries were 1.9 MPa/K for increasing p and 1.7 MPa/K for decreasing p , almost identical to those found for the 0.7 GPa phase lines. Also, the 0.3 GPa transition extrapolates to $T_u \pm 4$ K at $p = 0$, and we thus inferred at an early stage that the 0.3 GPa anomaly was identical to the ordering transition at T_u . Repeating the experiment at $T < 200$ K

to check this, however, revealed that the phase boundary curved out and away from the T axis, such that $dp/dT \rightarrow 0$ as $T \rightarrow T_u$.

The final phase boundary found is shown in Fig. 4. Different symbols denote different samples; open symbols denote passing through the phase line in the direction toward high p or low T , and filled symbols in the opposite direction. Both phases are stable in the hatched area, depending on past history. The very small slope dp/dT below 200 K is clearly evident in the figure, as is the fact that this "horizontal" phase line is joined by a "vertical" phase line to T_u at zero pressure. The slope dp/dT of the latter is, to within the experimental error, infinite. No anomalies in ρ were found except on the phase boundaries shown. This is demonstrated by curves D and E in Fig. 2, and by Fig. 5, which shows measured data for ρ along the trajectory $ABCD$ (indicated in Fig. 4), which carries us from the low- p or high- T phase into the medium- p or low- T phase, around the sharp bend in the phase line, and back into the first phase again. During the initial isobaric cooling at 170 MPa we find a transition at 190 K but no further anomalies. At 115 K (well below T_u at $p=0$) p is slowly decreased to 50 MPa. During this decrease no step (order-disorder) anomaly of the type shown in Fig. 1 is observed, although such anomalies are found at both increasing and decreasing p at any $T > 125$ K. However, there is a change in $d\rho/dp$ at approximately 90 MPa, corresponding to passing through the extrapolation of the lower phase line in Fig. 4, and similar to the corresponding change in $d\rho/dp$ at 150 MPa and 295 K (Fig. 1). At 50 MPa the sample is then heated to 137 K, again showing an anomaly in ρ at 125 K similar to that observed at 190 K. The similarity is shown more clearly by the final curve (triangles), which shows $\rho(T)$ during cooling at 30

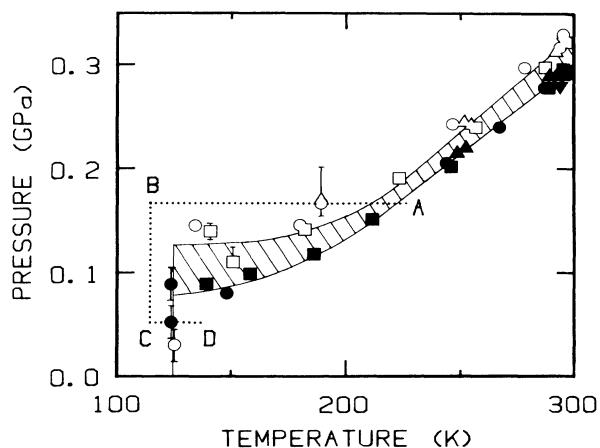


FIG. 4. Part of the p - T phase diagram for KC_{24} , showing the locations of all resistance anomalies corresponding to the T_u -low- p transition. Open symbols denote passing through the transition in the direction toward high p and low T , filled symbols the opposite direction. Different symbols denote data for different samples. Where no error bars are shown, the maximum error is smaller than the extent of the symbol. Resistance data measured along the dotted line $ABCD$ are shown in Fig. 5.

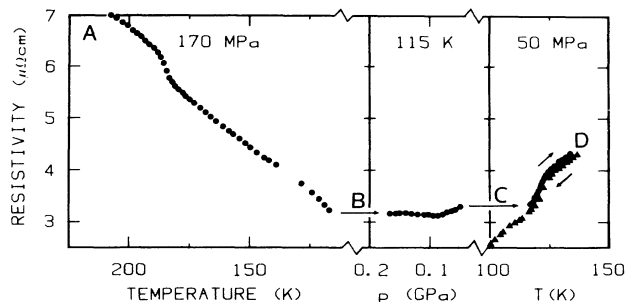


FIG. 5. Circles: Measured resistivity data along the trajectory $ABCD$ shown in Fig. 4, in chronological order from left to right. Triangles: Similar data for decreasing T at 30 MPa, taken immediately after reaching point D . Triangles have been displaced downward by $0.25 \mu\Omega \text{ cm}$ to increase readability.

MPa immediately after reaching point D . At 30 and 50 MPa there is no doubt that the anomaly observed corresponds to that at $T_u = 125$ K at 0.1 MPa.

The rather unusual phase diagram in Fig. 4 is in sharp contrast to that of the analogous compound³ LiC_{16} . At 0.1 MPa staging transitions (versus T) are never observed in KC_{24} , and the stable phase is pure stage 2, ordered below T_u and disordered above. The very large slope dp/dT of the phase boundary near T_u is then easily explained. For the ordering transition in the pure stage-2 phase the entropy change dS is large but the volume change dV quite small,²⁸ resulting in a very large slope $dp/dT = dS/dV$. The results in Fig. 4 then imply that no staging occurs at 125 K until at above 100 MPa. Above this the sample is⁷ a mixture of stage-2 material which, at least above T_u , is disordered, and stage-3 material. Since easily identified characteristic anomalies in ρ were always observed when crossing the phase boundary in Fig. 4, but nowhere else, and since the phase boundary is continuous, it is probable that the curved boundary also represents some kind of ordering phenomenon, probably the same in-plane K ordering within the stage-2 phase as below 100 MPa. However, there are other possibilities, such as a general in-plane ordering of all K atoms, a similar ordering within the stage-3 phase, or a change in the c -axis stacking sequence. The evidence available is:

(1) $\Delta\rho$ is independent of p and T , and identical to that found at the "vertical" boundary segment.

(2) The c -axis repeat distance of the stage-3 phase does not change significantly at the transition near 300 K. Figure 6(a) (adapted from Fig. 9 of Kim *et al.*⁷) clearly shows this. The c axis repeat distance of the stage-2 phase decreases by about 0.5%, and the resulting volume decrease leads to a much smaller value of $dp/dT = dS/dV$ here than near T_u .

(3) Figure 6(b) (adapted from Fig. 7 of Kim *et al.*⁷) shows a sharpening of the stage-2 diffraction peaks at the transition, indicating increasing order. The stage-3 peaks sharpen only gradually above the anomaly.

(4) On going through the extrapolated phase line below 120 K no step anomaly is found in ρ .

We conclude that the phase boundary in Fig. 4

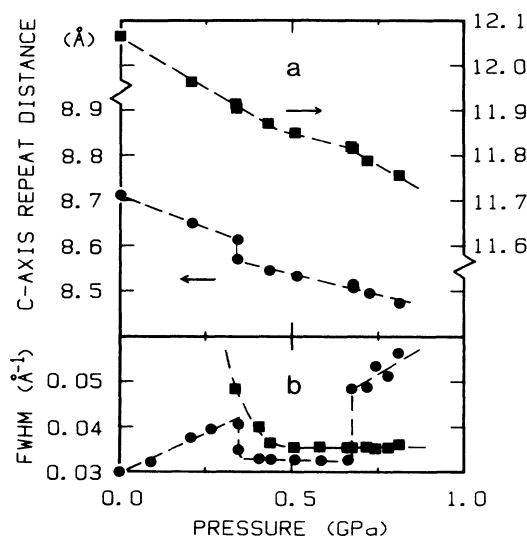


FIG. 6. (a) c -axis repeat distance vs p for stage-2 (circles, left-hand scale) and stage-3 (squares, right-hand scale) KC_{24} . (b) Diffraction peak width for stage-2 and -3 KC_{24} . Symbols as in (a). Both figures adapted after Kim *et al.* (Ref. 7).

represents the same intraplane ordering of the K atoms in the stage-2 phase as is seen at zero pressure near 125 K. However, we cannot tell whether a similar ordering occurs simultaneously in the stage-3 phase present. The in-plane structures of several originally stage-2 alkali metal GIC's have been studied under pressure,^{5,34,35} but there are no data for stage-3 KC_{24} below 0.3 GPa. Although KC_{24} , RbC_{24} , and CsC_{24} should behave similarly under pressure they certainly do not behave identically. For example, the "floating solid" type phase found by Wada *et al.*³⁴ in CsC_{24} has never been observed in KC_{24} , and we shall not extrapolate results for Rb and Cs GIC's to the present case. However, it is reasonable to expect the densely packed stage-3 phase always to be ordered.

We summarize the results of Secs. III C and III D as follows. Above 150 K, KC_{24} is a pure disordered stage-2 material at 0.1 MPa, while above 100 MPa it is a mixture⁷ of disordered stage 2 and 0–40% (ordered?) stage 3. At 0.15–0.33 GPa the stage-2 (and -3?) phase orders, and above this the sample is a mixture of ordered stage-2 and -3 materials. The strain energy released as the c -axis repeat distance decreases on ordering [Fig. 6(a)] allows a simultaneous conversion⁷ of some stage 2 into stage 3. Depending on T , the staging transition finally goes to completion at 0.6–0.7 GPa. Below 125 K, on the other hand, the absence of anomalies in ρ indicates that both the stage 2 and the stage-3 phases are always ordered, from 0.1 MPa up to and above the start of the staging transition. The breaks in $\rho(p)$ in Figs. 1 and 5 might indicate that the latter starts at approximately the same p (≈ 100 MPa) at 115 and 295 K.

E. Phase boundary for the ordering transition at T_1 , and the low- T and/or high- p corner of the KC_{24} phase diagram

Although T_1 is well below the freezing temperature of the pressure medium we were able to trace the transition anomaly to above 0.5 GPa by making isobaric measurements of $\rho(T)$. The anomaly in ρ was always well defined and the hysteresis in T small. No attempt was made to observe any t dependence. The phase boundary found is shown in Fig. 7, which shows all transition points found in the p - T plane for KC_{24} using the same symbols as Fig. 4. The points denoting the transition at T_1 are distinguished from those denoting the staging transition by a small star inside the symbol.

The transition at T_1 affects the stage-2 phase only. This is shown by curve C in Fig. 2, obtained by completing the staging transition at 245 K, then cooling to 105 K within the stage-3 phase without finding any anomalies in ρ . Repeated isobaric runs between 100 and 150 K at lower pressures revealed no anomalies until after crossing the lower phase boundary for the stage-3 phase (~ 0.4 GPa at 150 K), when a large anomaly ($\Delta\rho/\rho \approx 0.07$) immediately appeared. Identical anomalies were always observed for $p < 0.4$ GPa. Increasing p again up through the staging transition at $T < 150$ K, however, a small anomaly in ρ always remained even within the stage-3 phase, indicating the presence of some metastable stage-2 phase. This is indicated by the dashed high- p extension of

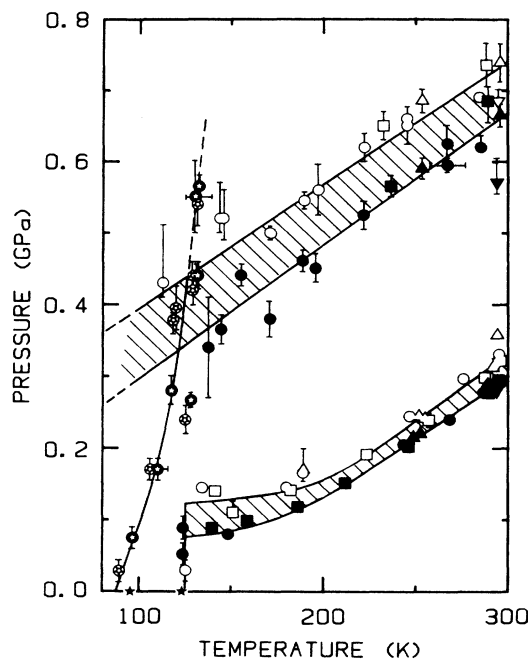


FIG. 7. p - T phase diagram for KC_{24} , showing the location of all resistance anomalies identified. Symbols are the same as in Fig. 4, except that the stars at $p=0$ indicate T_1 and T_u from Ref. 9, and that the transition at T_1 is indicated by a small star in each symbol.

the T_l phase line (and the corresponding points) in Fig. 7. No significant difference was observed between anomalies obtained after increasing p at temperatures above or below the T_l phase line, respectively, at $T < 150$ K, but crossing the "staging" phase line at higher temperatures led to a rapid decrease in the size of the (metastable) T_l anomaly. We conclude that the staging transition always goes to completion [$>95\%$ (Refs. 7 and 33) stage 3] at $T > 245$ K but that sizeable amounts of the low- p stage-2 phase remain after pressurizing below 150 K. This may be due either to the non-hydrostatic pressure at these temperatures or to limited kinetics in the transition at low T . The slope of the T_l phase line is approximately 7.5 MPa/K at low p but seems to increase at higher pressures. This is probably an experimental artifact due to the scatter in the measured transition temperatures, but could possibly be connected with the increasing amount of stage-3 phase with increasing p .

There is some uncertainty as to whether there is still a staging transition below 140 K. In Fig. 7, the phase line for the staging transition extends to lower temperatures and there is a triple point at 125 K/0.45 GPa (neglecting metastability effects). However, we cannot safely distinguish between the diagram shown and a behavior similar to that for the lower transition, with a sharp downward break in the phase line down to T_l , since the solidification of the pressure medium made it impossible to obtain reliable data for $\rho(p)$ below 130 K. We made two isothermal measurements of $\rho(p)$ near 110 K, and in both cases we found a sharp apparent increase in ρ between 0.4 and 0.45 GPa. However, these features may have been due simply to nonhydrostatic strain in the coil system. These measurements are represented by a common point at 110 K in Fig. 7. A second indication of low- T staging is obtained from plots of ρ versus p at 110 K, as obtained from the isobaric measurements of $\rho(T)$. At $p > 0.4$ GPa ρ is linear in p with a negative slope $d\rho/dp$ similar to that observed at 300 K, but at $p < 0.3$ GPa, ρ is significantly ($>5\%$) smaller than the extrapolated high- p value. Figure 7 thus gives the most probable phase boundary for this region.

We conclude Sec. III by stressing the fact that Fig. 7 is not a true phase diagram for KC_{24} showing equilibrium phases versus p and T , but only shows the p - T locations of the anomalies found in ρ . Also, the figure does not show the phase boundary pertaining to the start of the 2 \rightarrow 3 staging transition at low p discussed above.

IV. EXPERIMENTAL RESULTS AND DISCUSSION: STAGE-3 AND -4 K-GIC

A. Structures and phases transitions

The nominal compositions of stage-3 and -4 K-GIC's are KC_{36} and KC_{48} , respectively. At 300 K and 0.1 MPa the in-plane structures³⁶ are liquidlike and similar to that of KC_{24} , except for a slightly smaller in-plane K density. Two anomalies are observed⁹ in ρ for both materials at low T . For KC_{48} these are similar to those observed in KC_{24} , except that $T_u \approx 250$ K. For KC_{36} , however, only the lower anomaly is similar to those in KC_{24} and KC_{48} , while the upper anomaly at $T_u \approx 240$ K is only a smeared

increase in $d\rho/dT$. The actual transitions giving rise to the upper anomalies are³⁶ more or less continuous between 120 K and T_u and probably similar to that in KC_{24} . At high p both materials densify to closer packed, higher-stage compounds. KC_{36} transforms⁷ smoothly, starting near 0.1 MPa, from stage 3 to almost pure stage 4 at 0.65 GPa, the stage-4 phase persisting to approximately 0.75 GPa where the material abruptly transforms into mainly stage 5. The latter transition is probably associated with an in-plane densification to a close-packed 2×2 structure.³⁷ Both transitions are reversible with a hysteresis less than 0.1 GPa. KC_{48} behaves similarly,³⁷ transforming smoothly to stage 5 at 0.7 GPa, then abruptly turning into a mixed (mainly stage-6) close packed phase at 0.8 GPa. These staging transitions have been observed by Fuerst *et al.*⁶ as a number of anomalies in ρ_c under pressure.

B. Experimental results for KC_{36}

Three stage-3 samples were studied, one at high p at 295 K, and at 0.2 GPa down to 150 K, one between 295 and 245 K, and a third at 295 K only. The measured values of ρ were 4.7, 5.3, and 6.2 $\mu\Omega\text{cm}$, respectively, at STP, in excellent agreement with literature.^{9,20} Figure 8 shows $\rho(p)$ for increasing p for two samples, identified by different symbols. Sample 1 (dots) was studied at 295 K only while sample 2 (triangles) was also studied at 245 K. As for KC_{24} , the anomalies in ρ correlate well with both the anomalies in ρ_c (Ref. 6) and the known staging transitions under pressure.⁷ In contrast to the case of KC_{24} , ρ increases linearly with p up to 0.5 GPa, consistent with the smooth stage 3 \rightarrow 4 transition⁷ starting near 0.1 MPa.

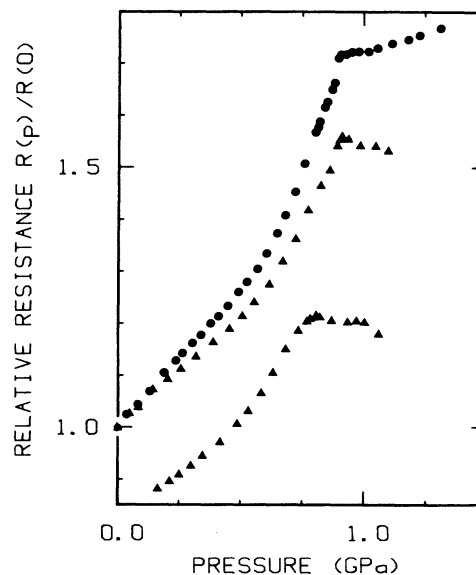


FIG. 8. Relative resistance $R(p)/R(0)$ for two KC_{36} samples, identified by different symbols. Upper two curves measured at 295 K, bottom curve at 245 K.

Above 0.5 GPa, ρ increases faster with p , until at about 0.75–0.8 GPa there is a 25% decrease in $d\rho/dp$ (hardly noticeable on the scale of the figure), which we suggest corresponds to the end of the 3→4 staging transition.⁷ At 0.85 to 0.89 GPa, depending on the sample, there was then a small final step increase in ρ , corresponding to the abrupt 4→5 staging transition.⁷ Above 0.9 GPa $d\rho/dp$ was positive for sample 1 but negative for the other two samples. No time dependence was observed in ρ at any p . Our values for the transition pressure are in fair agreement with the previous results 1.0 ± 0.05 GPa (Fuerst *et al.*⁶) and 0.79 GPa (Kim *et al.*⁷). The hysteresis was approximately 0.09 GPa at the 4→5 transition, decreasing to about 0.02 GPa at the 0.5 GPa “knee,” and thus similar to that found by Kim *et al.*⁷

The results obtained for the third sample at 295 K were in excellent agreement with those for sample 2 shown in the figure. The mean γ observed for the high-pressure stage-5 phase was very close to zero with an observed scatter from $+0.09$ to -0.06 GPa⁻¹. Using $k_c = 2.5 \times 10^{-2}$ GPa⁻¹ for stage-5 KC₃₆ from Kim *et al.*⁷ we obtain a corrected value $\gamma = -0.02$ GPa⁻¹, with an error given by the scatter, and a volume dependence $d(\ln\rho)/d(\ln V) \approx 1$. Using again the discussion in Sec. III C, with a γ_G value derived from Hardcastle and Zabel,²⁸ the corresponding theoretical value from Eq. (2) is in the range 0.5–1. In view of the large possible error, however, the good agreement with theory should not be taken too seriously. No data for $d\rho/dp$ can be obtained for either the stage-3 or stage-4 phases.

It is evident from the figure that $d\rho/dT$ is higher in the high- p phase than at 0.1 MPa, just as for KC₂₄. Figure 9 shows $\rho(T)$ down to 150 K for sample 1 at 0.2 GPa, and for sample 2 between 250 and 290 K at 0.35 and 1.02 GPa. For sample 1 we observe the T_u transition at 235 ± 10 K (arrow). From Figs. 8 and 9 and similar data we obtain the p - T phase diagram for KC₃₆ shown in Fig. 10. We indicate the positions of the 0.5 GPa “knee” and the 4→5 staging transition by various symbols, as for

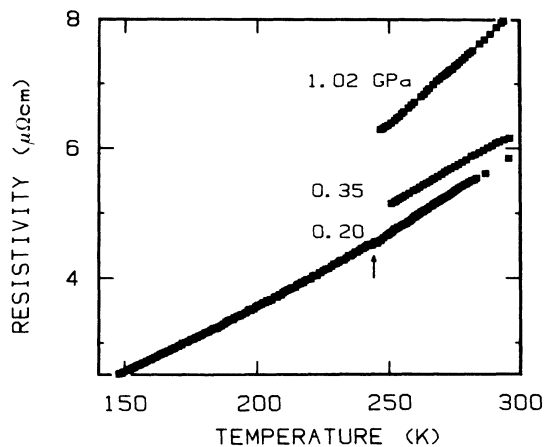


FIG. 9. Resistivity vs T for two KC₃₆ samples at the pressures indicated. Bottom curve sample 1, upper two curves sample 2.

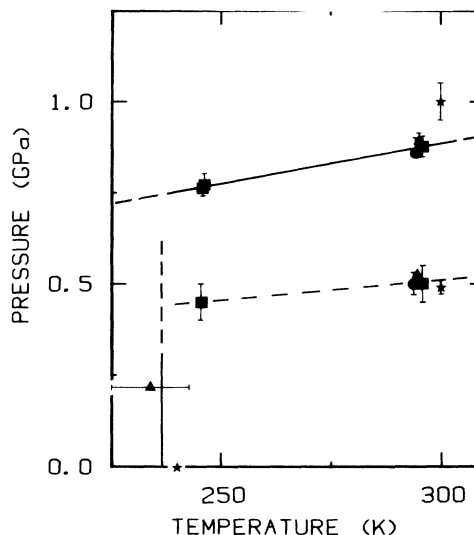


FIG. 10. Preliminary p - T phase diagram for KC₃₆. Symbols as in Fig. 7; the stars at 300 K show the results of Fuerst *et al.* (Ref. 6). See text for further details.

KC₂₄. Only transitions toward high- p are shown. The stars at $p=0$ and at $T=300$ K indicate the results by Onn *et al.*⁹ for T_u and by Fuerst *et al.*⁶ for the 0.5-GPa knee and 4→5 transition, respectively. The phase boundary for the 4→5 transition is shown by a line with a slope of 2.3 MPa/K; the transition extrapolates to ≈ 0.21 GPa at $T=0$. The phase boundary for T_u is shown as a vertical line. The linearity of $\rho(T)$ at 0.35 GPa down to 245 K (Fig. 9) puts a lower limit on the slope of this line at approximately 25 MPa/K. Since T_u indicates an ordering within the stage-3 phase this boundary probably ends at the stage 3→4 phase transition at ≈ 0.6 GPa.

From Kim *et al.*⁷ we know that an appreciable part of the material transforms into stage 4 at quite low pressures (<0.2 GPa). Since the slopes of the phase lines are fairly large, our data indicate that it is reasonable to expect a staging transition 3→4 (but not 4→5) at low T . Such a transition has not been reported to date.

C. Experimental results for KC₄₈

Only one KC₄₈ sample was studied, at 295 and at 247 K. At STP $\rho = 12.2$ $\mu\Omega$ cm, substantially higher than literature data.^{9,20} The high measured value must be caused by some microscopic flaw, since x-ray analysis characterized the sample as pure stage 4. Figure 11 shows $\rho(p)$ at 295 K. The results are quite similar to those for KC₃₆ and can be interpreted in the same way. The linear increase in ρ at low p , followed by an increase in $d\rho/dp$ at 0.55 ± 0.1 GPa probably indicates the smooth transition³⁷ from stage 4 to 5, while the sharp break at 0.98 ± 0.02 GPa signals the final abrupt transition to (mainly) stage 6. The hysteresis at 1 GPa was only about 0.05 GPa in this case, while no hysteresis at all was found for the 0.55 GPa “knee.” At 247 K, the two anomalies were found at 0.55 ± 0.05 GPa and 0.87 ± 0.01 GPa, and the slope of the

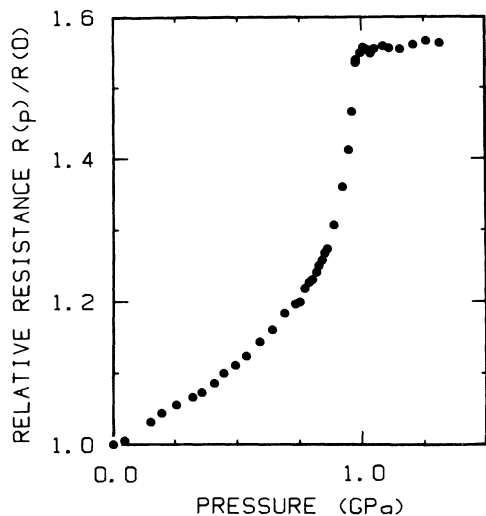


FIG. 11. Relative resistance $R(p)/R(0)$ vs p for KC_{48} .

5→6 transition boundary is thus 2.2 MPa/K. Both anomalies extrapolate to positive pressures at $T=0$, but since the staging transition actually starts³⁷ at low p we again expect a low T staging transition at 0.1 MPa which has not been observed to date.

$(1/\rho)d\rho/dT$ was 10% larger in the high- p phase than at 0.1 MPa, while γ in the high- p stage-6 phase was small and positive, $\gamma=0.02 \text{ GPa}^{-1}$, at 295 K, but zero at 247 K. The general behavior is thus similar to that for KC_{36} . No k_c data are available for the high- p phase. However, k_c should be $0.02\text{--}0.03 \text{ GPa}^{-1}$, making the true γ small and negative with $d(\ln\rho)/d(\ln V)$ between 0 and 1. Extrapolating the data of Hardcastle and Zabel²⁸ to KC_{48} we find a theoretical value from Eq. (2) of $d(\ln\rho)/d(\ln V)\approx 0.5$, in good agreement with the experimental result. As noted in Sec. III C, however, this does not necessarily indicate that electron-phonon scattering dominates over band-structure effects under pressure.

V. CONCLUSIONS: p - T PHASE DIAGRAMS OF K-GIC'S

A large amount of data has been collected on phase changes in the p - T plane for stage 2–4 K-GIC's. All these materials have some general features in common. Staging transitions are not observed at low T and atmospheric pressure, but increasing p by < 100 MPa at 300 K immediately initiates such a transition. The p - T loci of anomalies in ρ induced by staging imply that a large part of these staging transitions should appear at 0.1 MPa at some $T > 0$ K. These features contrast sharply with the simple phase diagram found from $\rho_c(p, T)$ and x-ray diffraction for the Li-GIC system.³ Some possible explanations for this anomalous behavior were discussed previously,¹³ and we shall here summarize that discussion together with the new information available from this work.

Staging transitions are usually discussed in terms of the Daumas-Hérolde (DH) model,²⁵ in which it is assumed

that the number of intercalant atoms is roughly the same in every graphite gallery in the GIC crystal. A well-defined stage number is still obtained if the crystal is assumed to consist of many small columnar domains, each of which is well staged but with adjacent domains not having the same graphite galleries filled. Staging transitions then easily occur through local in-plane sliding of intercalate islands between adjacent domains, in general accompanied by simultaneous densification within each intercalate layer. The details of this process, however, are not yet known, although a great deal of work is presently being done on this subject.³⁸

We recently suggested¹³ that the unusual phase diagram of KC_{24} , and the difference between the K- and Li-GIC's, is the result of interaction between the DH domain walls and the intraplane discommensuration or domain structure¹⁸ at low T . Each DH domain probably contains many locally commensurate regions bounded by discommensuration boundaries must pass through each DH domain boundary, which can be considered as an array of dislocations, and we argued that this movement is hindered by the discommensuration walls being pinned by dislocations at the domain boundaries at low T . The in-plane graphite corrugation potentials for the alkali metals has been estimated by DiVincenzo and Mele,³⁹ who found barrier heights for motion between adjacent hexagonal sites of about $40kT$ for Li and $3\text{--}4 kT$ for the other alkali metals. Li-GIC's therefore form commensurate structures more readily than K-GIC's, despite the fact that the in-plane kinetics of Li-GIC's are much slower. For K-GIC's in-plane ordering occurs on a time scale of minutes at $T\approx 130$ K, while for Li-GIC's the ordering and staging transition at 240 K takes days to complete. Although the atomic diffusivity in K-GIC's is thus large enough for locally commensurate regions to quickly form at T_u , these regions themselves have effectively zero diffusivity at low T due to pinning at the DH domain walls, and no staging transition can occur in K-GIC's at low T .

An alternative explanation may be inferred from a recent experiment of Winokur and Clarke.¹² They find that the discommensuration-domain structure breaks up below T_l into at least four different commensurate "microphases," each with different areal densities of K atoms. By varying the relative amounts of such phases this mechanism could stabilize an average in-plane $[\text{K}]/[\text{C}]$ ratio near $\frac{1}{12}$, regardless of the actual stoichiometry, and thus remove the driving force for a staging transition. However, other recent experiments¹⁹ suggest that this may not always be the case. Stage-2 samples with different $[\text{K}]/[\text{C}]$ ratios show subtly different T dependence in x-ray 00 l profiles, suggesting that at low $[\text{K}]/[\text{C}]$ ratios stage-3 packages may be formed at low T simultaneously with the formation of Winokur-Clarke microphases.

The new results presented here also allow a third explanation. The fact that staging in KC_{24} always seemed to start at > 0.1 GPa led us to suggest¹³ that staging was kinetically hindered at low T . However, the very low p necessary to initiate staging in KC_{36} and KC_{48} at 300 K, together with large phase boundary slopes at high p , suggests that staging may actually rather be kinetically hin-

dered at low p . This ties in well with the observation of a break in $d\rho/dp$ at 0.1 GPa in KC_{24} at 295 K, together with the vertical phase boundary near T_u : There is no staging transition until at ≈ 0.1 GPa, almost independent of T . This behavior could be explained in terms of the p dependence of the graphite corrugation potential: At low p , the potential is rather weak in K (as well as Rb and Cs) GIC's,³⁹ resulting in a liquidlike intraplane structure at high T . Cooling through T_u , the decrease in thermal energy coupled with phonon interactions⁴⁰ allows the formation of locally commensurate regions bounded by discommensurations, as discussed above, but no truly commensurate phase can be formed until below¹² T_l . As discussed in Sec. III E, we do not know whether there is still a staging transformation below T_l ; the formation of microphases¹² might inhibit staging completely. Increasing p , however, the corrugation potential increases as the graphite matrix is compressed. Taking KC_{24} as an example, at about 0.1 GPa the potential is large enough to allow formation of a truly commensurate 2×2 phase, and thus a stage-3 material. The increased potential will also make formation of the ordered stage-2 phase easier, explaining the sudden break in the phase line and the constant- p ordering between 125 and 200 K.

We thus have three different possible models for the mechanism behind the low- T -high- p behavior of K-GIC's. The available data, however, are not sufficient to allow us to identify which of these (or which combination of these) is truly responsible for the observed behavior. Obviously, the phase diagrams presented here are not truly phase diagrams; they give an indication of what hap-

pens when stage- n K-GIC is cooled or compressed but they do not show the equilibrium phase at each p and T . (For example, in no case do we show the lower phase limit for the high- p high-stage phase, since this is not known.) The phase diagrams should be investigated further by structural studies throughout the p - T plane. Of particular interest would be low-pressure studies up to 0.2 GPa at temperatures down to well below 100 K to study the temperature dependence of the start of the staging transitions in the various materials. In view of the slow kinetics, and the possibilities of metastability under nonhydrostatic pressures (see Sec. III E), such studies should preferably be made under truly hydrostatic pressures such as in He gas. Such studies might also resolve the question whether stage-3 KC_{24} is ordered below the 0.33-GPa stage-2 ordering transition. A second interesting possibility would be to determine whether there exists a $\sqrt{7} \times \sqrt{7}$ commensurate phase in the low stage potassium GIC's in any p - T regime, since there is evidence⁴¹ that this is the low- T ground-state of high-stage K-GIC's.

ACKNOWLEDGMENTS

We acknowledge useful discussions with Paul Heiney and Victoria Cajipe. We thank Arthur Moore of Union Carbide Corporation for providing the HOPG. This work was supported by the Swedish Natural Science Research Council and by the National Science Foundation—Materials Research Laboratory Program, Grant No. DMR85-19059.

¹S. A. Solin, *Adv. Chem. Phys.* **49**, 455 (1982).

²R. Clarke and C. Uher, *Adv. Phys.* **33**, 469 (1984).

³D. P. DiVincenzo, C. D. Fuerst, and J. E. Fischer, *Phys. Rev. B* **29**, 1115 (1984).

⁴B. Lundberg and B. Sundqvist, *Solid State Commun.* **58**, 747 (1986).

⁵R. Clarke, N. Wada, and S. A. Solin, *Phys. Rev. Lett.* **44**, 1616 (1980).

⁶C. D. Fuerst, D. Moses, and J. E. Fischer, *Phys. Rev. B* **24**, 7471 (1981).

⁷H. J. Kim, J. E. Fischer, D. B. McWhan, and J. D. Axe, *Phys. Rev. B* **33**, 1329 (1986).

⁸P. Hawrylak and K. R. Subbaswamy, *Phys. Rev. B* **28**, 4851 (1983); H. Miyazaki, Y. Kuramoto, and C. Horie, *J. Phys. Soc. Jpn.* **53**, 1380 (1984).

⁹D. G. Onn, G. M. T. Foley, and J. E. Fischer, *Phys. Rev. B* **19**, 6474 (1979).

¹⁰J. B. Hastings, W. D. Ellenson, and J. E. Fischer, *Phys. Rev. Lett.* **42**, 1552 (1979).

¹¹F. Rousseaux, R. Moret, D. Guérard, P. Lagrange, and M. Lelaurin, *J. Phys. Lett.* **45**, L1111 (1984); *Synth. Met.* **12**, 45 (1985); *Ann. Phys. (Paris) Colloq.* **11**, C2-85 (1986).

¹²M. J. Winokur and R. Clarke, *Phys. Rev. B* **34**, 4948 (1986).

¹³B. Sundqvist and J. E. Fischer, *Phys. Rev. B* **34**, 3532 (1986).

¹⁴B. Sundqvist and B. Lundberg, *Mater. Res. Soc. Res. Symp.* **22**(Pt. III), 281 (1984).

¹⁵B. Sundqvist and B. Lundberg, *J. Phys. C* **19**, 6915 (1986).

¹⁶D. E. Nixon and G. S. Parry, *J. Phys. D* **1**, 291 (1968).

¹⁷K. Phan, C. D. Fuerst, and J. E. Fischer, *Solid State Commun.* **44**, 1351 (1982).

¹⁸M. Suzuki, *Phys. Rev. B* **33**, 1386 (1986); H. Zabel, *Physica* **136B**, 1 (1986); R. Clarke, J. N. Gray, H. Homma, and M. J. Winokur, *Phys. Rev. Lett.* **47**, 1407 (1981).

¹⁹V. B. Cajipe and J. E. Fischer (private communication).

²⁰E. McRae, D. Billaud, J. F. Maréché, and A. Hérold, *Physica* **99B**, 489 (1980); E. McRae and J.-F. Maréché, *J. Phys. C* **18**, 1627 (1985).

²¹S. Kirkpatrick, *Rev. Mod. Phys.* **45**, 574 (1973).

²²B. Sundqvist and B. Lundberg, *J. Phys. C* **17**, L133 (1984).

²³T. Inoshita and H. Kamimura, *Synth. Met.* **3**, 223 (1981).

²⁴S. E. Ulloa and G. Kirczenow, *Phys. Rev. Lett.* **56**, 2537 (1986).

²⁵N. Daumas and A. Hérold, *C. R. Acad. Sci.* **268**, 373 (1969); G. Kirczenow, *Phys. Rev. Lett.* **52**, 437 (1984); *Synth. Met.* **12**, 143 (1985); *Phys. Rev. B* **31**, 5376 (1985); S. E. Ulloa and G. Kirczenow, *ibid.* **33**, 1360 (1986).

²⁶J. M. Ziman, *Electrons and Phonons* (Oxford University Press, Oxford, 1960), p. 419.

²⁷D. A. Benson and W. B. Gauster, *Philos. Mag.* **31**, 1209 (1975).

²⁸S. E. Hardcastle and H. Zabel, *J. Phys. (Paris) Colloq.* **C6**, C6-326 (1981).

- ²⁹K. Noto and T. Tsuzuku, *J. Phys. Soc. Jpn.* **35**, 1649 (1973); I. L. Spain, *Carbon* **14**, 229 (1976).
- ³⁰M. E. Potter, W. D. Johnson, and J. E. Fischer, *Solid State Commun.* **37**, 713 (1981).
- ³¹L. E. DeLong and P. C. Eklund, *Synth. Met.* **5**, 291 (1983); L. E. DeLong, V. Yeh, V. Tondiglia, P. C. Eklund, S. E. Lambert, and M. B. Maple, *Mater. Res. Soc. Symp. Proc.* **20**, 195 (1983).
- ³²B. Sundqvist, J. Neve, and Ö. Rapp, *Phys. Rev. B* **32**, 2200 (1985), and references therein.
- ³³H. J. Kim and J. E. Fischer, *Phys. Rev. B* **33**, 4349 (1986).
- ³⁴N. Wada, S. Minomura, and J. Pluth, *Synth. Met.* **12**, 51 (1985).
- ³⁵N. Wada, *Phys. Rev. B* **24**, 1065 (1981).
- ³⁶M. Mori, S. C. Moss, and Y. M. Jan, *Phys. Rev. B* **27**, 6385 (1983).
- ³⁷H. J. Kim, dissertation, University of Pennsylvania, 1986 (unpublished).
- ³⁸G. Forgács and G. Uiman, *Phys. Rev. Lett.* **52**, 633 (1984); M. E. Misenheimer and H. Zabel, *ibid.* **54**, 2521 (1985); P. Bak and G. Forgács, *Phys. Rev. B* **32**, 7535 (1985); G. Kirczenow, *Phys. Rev. Lett.* **55**, 2810 (1985).
- ³⁹D. P. DiVincenzo and E. J. Mele, *Phys. Rev. Lett.* **53**, 52 (1984); *Phys. Rev. B* **32**, 2538 (1985).
- ⁴⁰C. Horie, H. Miyazaki, S. Igarashi, and S. Hatekeyama, *J. Phys. (Paris) Colloq.* **C6**, C6-298 (1981); C. Horie, S. A. Solin, H. Miyazaki, S. Igarashi, and S. Hatekeyama, *Phys. Rev. B* **27**, 3796 (1983); W. A. Kamitakahara and H. Zabel, *ibid.* **32**, 7817 (1985); H. A. Zabel, M. Suzuki, D. A. Neumann, S. E. Hardcastle, A. Magerl, and W. A. Kamitakahara, *Synth. Met.* **12**, 105 (1985); D. P. DiVincenzo, *ibid.* **12**, 111 (1985).
- ⁴¹P. A. Heiney, M. E. Huster, V. B. Cajipe, and J. E. Fischer, *Synth. Met.* **12**, 21 (1985).